Effects of Hydrothermal-Chemical Treatments on Bending Performance and Physical-Mechanical Properties of Four Timber Species

Huajie Shen , A. Caixia Bai , A. Fengwu Zhang, Yue Sun, A. Xinzhen Zhuo, A. Rongfeng Ding, A. Donghai Huang, A. Yushan Yang, A. and Jian Qiu

The bending behavior of four key timber species (*Fraxinus chinensis*, teak, rubberwood, and *Pinus yunnanensis*) was evaluated under hydrothermal-chemical treatments. Controlled experiments at varying moisture contents (20 to 60%), temperatures (100 to 140 °C), and treatment durations (4 to 8 h) revealed that bending strength and elastic modulus decreased by 18 to 32% with increased moisture and temperature, stabilizing beyond critical thresholds (40% moisture, 120 °C). Among the treatments, the compound lye (40% ammonia + 5% ethylenediamine with surfactants) outperformed ammonia and water treatments, achieving the highest bending deformation height-to-radius ratio of 0.102. X-ray diffraction and Fourier-transform infrared spectroscopy analyses confirmed selective lignin degradation and reduced inter-fiber friction. These findings suggest that this method offers a promising, cost-effective approach for improving the structural integrity of curved wood components.

DOI: 10.15376/biores.20.2.4635-4661

Keywords: Wood bending; Three-point bending test; Chemical modification; Elastic modulus

Contact information: a: School of Design, Fujian University of Technology, Fuzhou, Fujian 350118, China; b: Fujian University of Technology Intangible Cultural Heritage Arts and Crafts Research Center, Fuzhou, Fujian 350118, China; c: School of Mechanical and Electrical Engineering, Sanming University, Sanming, Fujian 365004, China; d: School of Materials and Chemical Engineering, Southwest Forestry University, Kunming, Yunnan 65224, China;

* Corresponding authors: shenhuajie@fjut.edu.cn; ysyoung@swfu.edu.cn; qiujian@swfu.edu.cn

INTRODUCTION

Wood, as a widely used natural material in construction, furniture manufacturing, and industrial products, has mechanical properties that are crucial to its performance and range of applications (Mai *et al.* 2022). The bending performance of wood, especially in static three-point bending tests, is an important indicator for evaluating its mechanical properties. The bending performance of wood is influenced not only by the wood species, structural characteristics, and moisture content, but also closely related to its density, fiber arrangement, and cellular structure (Fajdiga *et al.* 2019; Ratnasingam *et al.* 2022). Therefore, in-depth research on the bending performance of different wood species and the factors that affect it is of great theoretical and practical significance for the processing, use, and optimization of wood (Perçin *et al.* 2024).

In wood mechanics research, softening treatments are common processing methods that can significantly alter the internal structure and physical properties of wood, thereby enhancing its workability and subsequent durability (Wu *et al.* 2022). By using different softening agents and treatment processes, the density, cellular structure, and stress

distribution of wood can change, affecting its mechanical properties (Aramburu *et al.* 2022). In particular, during hydrothermal treatment and chemical softening, the choice of softening agents and processing parameters (such as temperature, time, and concentration) play a decisive role in the final properties of wood.

Although existing studies have explored the bending performance of wood and its influencing factors, there is still a lack of systematic analysis on the comparative bending performance of different wood species under the same treatment conditions, the optimization of softening methods, and the relationship between microstructure and mechanical properties. This study aimed to systematically evaluate the bending performance of four wood species (Chinese ash: *Fraxinus chinensis*; teak: *Tectona grandis*; rubberwood: *Hevea brasiliensis*; and Yunnan pine: *Pinus yunnanensis*) under different softening treatments using static three-point bending tests. The study combines physical and mechanical testing with anatomical analysis of wood to explore the comprehensive effects of wood species and treatment methods on the bending performance, with a particular focus on wood density, fiber structure, and their impact on bending strength.

The innovation of this study lies in comparing the bending performance of four wood species under different softening agent treatments, revealing the interrelationship between wood density, anatomical characteristics, and softening treatments, and providing experimental evidence for wood processing and performance optimization. The results not only help improve the performance of wood but also provide theoretical support for the improvement and optimization of related wood treatment technologies. This study not only provides a comparative analysis of the bending performance of four wood species under different softening treatments but also offers practical insights for optimizing wood processing techniques in industrial applications.

Background and Motivation

Recent research on wood softening technologies has gradually shifted towards the synergistic effects of chemical modification and physical treatments. For instance, Huang *et al.* (2024) explored the effects of hydrothermal – microwave treatment on the bending properties of plantation *T. grandis*. They found that combining water heat and microwave softening could achieve better softening effects than using either method alone, indicating a trend towards integrating physical and chemical approaches in wood softening processes. However, overtreatment may cause the wood to soften, thereby reducing its bending strength (Gašparík and Barcík 2014).

Regarding ammonia gas modification, Zhang *et al.* (2021) demonstrated that ammonia fumigation of *Betula alnoides* wood enhanced color variation, reduced wettability, and increased cellulose crystallinity by diminishing hydroxyl/carboxyl groups, highlighting ammonia's role in chemical modification for aesthetic and functional improvements. In a complementary study, Gao *et al.* (2023) explored gaseous ammonia coupled with heat treatment (180 °C, 6 h) on spruce wood, revealing that ammonia neutralized acidic byproducts from hemicellulose degradation, preserved cell-wall polymers, and restored mechanical properties (*e.g.*, modulus of elasticity, compressive strength) to near-native levels while minimally affecting equilibrium moisture content. Both studies emphasize that ammonia-based treatments optimize wood performance by altering chemical composition and microstructure, with process parameters (concentration, temperature) critically determining outcomes. Compared to room-temperature ammonia methods (Weigl *et al.* 2012), the integration of ammonia with high-temperature processing mitigates mechanical degradation typical of conventional heat treatment, offering a novel

green strategy for functional wood modification.

In the field of chemical modification, Xia *et al.* (2018) employed a choline chloride/glycerol binary deep eutectic solvent (DES) to treat wood, but its ability to cleave lignin ether bonds remained limited. Bai *et al.* (2024) innovatively constructed a lactic acid/choline chloride/FeCl₃ ternary DES system, which significantly enhanced lignin removal efficiency while maintaining 77.1% cellulose retention through the synergistic strengthening of hydrogen bond intensity via Fe³⁺ acidic sites. This ternary DES disrupted lignin's hydrogen bonds and ether bonds, thinning wood cell walls and creating a porous network structure (as revealed by SEM analysis). Consequently, it improved material flexibility (with fracture displacement reaching 20 mm) and tensile resilience (exhibiting 7.3% fracture elongation rate). Yang *et al.* (2019) demonstrated that compound lyes (ammonia + ethylenediamine + surfactants) synergistically degrade lignin and hemicellulose while lubricating fiber interfaces, achieving a 45% reduction in fiber fracture during bending.

Tong *et al.* (2013) systematically investigated the longitudinal compression characteristics and multi-directional bending behaviors of juvenile and mature elm wood after hydrothermal treatment. The study demonstrated that this treatment significantly enhanced cellulose crystallinity in both wood types while enabling multi-directional bending capability. Kherais *et al.* (2024) investigated the influence of moisture content on the mechanical properties of timber structures. Three test groups, each containing 30 specimens, were subjected to four-point bending tests. The results demonstrated that increased moisture content led to variations in both elastic modulus and modulus of rupture. Additionally, the material behavior of some specimens transitioned from brittle to semi-ductile or ductile characteristics.

Recent methodological innovations in wood bending research integrate computational modeling with experimental validation (Kubík *et al.* 2024), nondestructive testing with standardized protocols (Kurul and As 2024), and statistical-environmental controls (Pestka *et al.* 2019; Hussin 2023). These approaches address wood orthotropy modeling, MOE/Modulus of Rupture (MOR) variations, and mechanical consistency quantification through linear approximations of stress-strain relationships. However, their application to chemically modified wood — particularly hydrothermal-alkali treated specimens—remains unexplored, especially regarding rate-dependent failure modes under combined hygro-thermal-mechanical stresses.

EXPERIMENTAL

Materials

To minimize the impact of wood variability, this experiment selected flawless mature heartwood from four important timber species: teak (*Tectona grandis*), Chinese ash (*Fraxinus chinensis*), rubberwood (*Hevea brasiliensis*), and Yunnan pine (*Pinus yunnanensis*), with a transverse section radial angle of no more than 10° and a grain angle controlled below 30° . All four timber species were sourced from Pu'er City, Yunnan Province, and were aged between 15 and 20 years. The initial size of each wood specimen was 1000 mm (length) $\times 40 \text{ mm}$ (width) $\times 20 \text{ mm}$ (height). Through precision longitudinal cutting (length adjustment: $1000 \rightarrow 300 \text{ mm}$) and lateral dimensioning (width reduction: $40 \rightarrow 20 \text{ mm}$), the final test specimen dimensions of $300 \text{ mm} \times 20 \text{ mm} \times 20 \text{ mm}$ were achieved. The original 20 mm height dimension was preserved, with surface polishing

limited to <0.1 mm material removal (GB/T 1936.1-2009 compliant) to ensure smoothness (Ra \leq 3.2 μ m) while maintaining nominal thickness.

The following chemical reagents were used (Table 1): deionized water, ammonia (25 to 28%(GR), Aladdin, China), ethylenediamine (≥99.5%(GC), Aladdin, China), lignosulphonate (99.9%, Aladdin, China), polyethylene glycol 200 (Purity: CP, GR, Aladdin, China), sodium dioctyl sulfosuccinate (≥96%, Klamar, China), fatty alcohol polyoxyethylene ether AEO-3 (99%, Macklin, China), alkylphenol polyoxyethylene ether TX-10 (99%, Klamar, China), and glacial acetic acid (99%, Aladdin, China), all of which were of analytical grade.

Preparation of the Softening Agent Sample Preparation

This study used three types of softeners: compound alkali solution, ammonia solution, and water. For water treatment and ammonia water treatment, no preparation was required. The preparation process of the compound alkali solution was as follows:

First, mix a 25% ammonia solution with 5% ethylenediamine. Then, add an appropriate amount of lubricant, swelling agent, dispersant, and surfactant, specifically: 4% lignosulfonate, 2% polyethylene glycol 200, 1% sodium dioctyl sulfosuccinate, 0.8% fatty alcohol polyoxyethylene ether AEO-3, 0.4% alkylphenol polyoxyethylene ether TX-10, and 0.5% glacial acetic acid. Afterward, add deionized water to the mixture to form a uniform compound softener solution. It is important to note that the proportion of ammonia solution and ethylenediamine should not exceed 30% of the total liquid volume of the softening agent. Once the ammonia-based softener is compounded, a new compound alkali solution is obtained.

Table 1. Chemical Reagents Used in the Experiment

Drug Name	Molecular Formula	Molecular Weight	Melting Point	Boiling Point (760 mmHg)	Flash Point	
Deionized water	H ₂ O	18.015	0 ℃	100.0±9.0 °C	100 °C	
Ammonia water	NH ₃ ·H ₂ O	35.046	-77 °C	36 °C	N/A	
Ethylene Diamine	$C_2H_8N_2$	60.098	8.5 °C	119.7±8.0 °C	33.9±0.0 °C	
Glacial acetic acid	СН₃СООН	60.052	16.2 °C	117.1±3.0 °C	40.0±0.0 °C	
Absolute ethanol	C ₂ H ₆ O	46.068	-114 ºC	72.6±3.0 °C	8.9±0.0 °C	
Safranine O	C ₂₀ H ₁₉ N ₄ CI	350.84	N/A	N/A	46 °C	
Sodium lignosulfonate	C ₂₀ H ₂₄ Na ₂ O ₁₀ S ₂	534.508	1704 °C	993 °C	N/A	
Polyethylene glycol 200	[CH ₂ -O-CH2]n	190-210	250 °C	65 °C	171 °C	
Sodium dioctyl sulfosuccinate	C ₂₀ H ₃₇ NaO ₇ S	444.558	N/A	N/A	N/A	
Fatty alcohol polyoxyethylene ether AEO-3	RO-(CH ₂ CH ₂₀)n-H	N/A	N/A	N/A	N/A	
Alkylphenol ethoxylate TX-10	C ₃₃ H ₆₀ O ₁₀	616.823	N/A	662.124 °C	354.24 °C	

Anatomical Characteristics

Approximately 10 mm × 10 mm × 10 mm fresh wood blocks were taken from each tree species for water-boiling softening (the boiling time depends on the hardness of the test material). After proper softening, the wood blocks were thoroughly rinsed with cold water for 3 to 5 times. Then they were prepared as slices with thicknesses of 12 to 20 μm on the transverse, radial, and chordal planes using a Leica SM 200R sliding microtome (Leica Microsystems GmbH, Germany). The obtained slices were stained in a 50% Safranine O solution for 24 h, then dehydrated with various concentrations of ethanol aqueous solution, and treated with xylene for transparency and cleanliness. Finally, the slices were sealed with neutral gum, labeled, and dried. According to the IAWA hardwood classification standard (Schweingruber and Crivellaro 2016), the slices were observed and measured using a Nikon biological digital microscope image analyzer (CELIPSE 80i, Nikon, Japan).

Softening Modification Treatment

Sample drying and weighing

The wood samples (300 mm \times 20 mm \times 20 mm) were dried in an oven at 103 °C until they reached a constant weight, ensuring all moisture was removed, before recording the initial dry weight.

Softening treatment

In Experiment (1), the samples were immersed in three different softening agents, with moisture content controlled at 20%, 30%, 40%, 50%, and 60%. The hydrothermal treatment was conducted at 120 $^{\circ}$ C for 6 h to ensure the stability of the treatment at the specified temperature.

In Experiment (2), the samples were immersed in three different softening agents, with moisture content set to 40%. Hydrothermal temperatures were set to 100, 110, 120, 130, and 140 °C, with a treatment time of 6 h, aiming to investigate the effect of varying temperatures on softening.

In Experiment (3), the samples were immersed in three different softening agents, with moisture content set to 40%. Hydrothermal treatment was conducted at 120 °C, with treatment times of 4, 5, 6, 7, and 8 h, to assess the influence of treatment duration on wood performance.

Softening treatment process

After each softening treatment, all soaked samples were wrapped in plastic film to prevent contamination or moisture loss during subsequent handling. The wrapped samples were then placed in a vertical pressure steam sterilizer (BOXUN, Shanghai Boxun Industrial Co., Ltd.) for steam softening treatment. The temperature and pressure during the softening process were maintained at stable levels to ensure uniform softening of the wood.

Performance measurement

After the softening treatment, the bending performance of the wood, including bending strength and elastic modulus, was measured. Additionally, the physical properties of the wood, such as density, shrinkage, and moisture absorption, were assessed to comprehensively evaluate the changes in wood performance after softening treatment.

Static Three-Point Bending Test of Wood Specimens

The experiment used the following equipment: digital display electronic thermostatic water bath (Guohua HH-4, Jiangsu Changzhou Guohua Electric Appliance Co., Ltd.), electric thermostatic oven (Guangming DHP-500, Beijing Xinrun Corona Instrument Co., Ltd.), biological digital microscope (Nikon 80i, Shanghai Puhua Optoelectronic Technology Co., Ltd.), digital display blast drying oven (GZX-9240 MBE, Shanghai Huyue Ming Scientific Instrument Co., Ltd.), and electronic digital vernier caliper (Mitech 150T, Germany Mitech Electronics). The basic physical properties of wood from different tree species, such as density, drying shrinkage coefficient, water absorption, and wet expansion, were measured according to the standards GB/T 1933-2009 (2009), GB/T 1932-2009 (2009), GB/T 1934.1-2009 (2009), and GB/T 1934.2-2009 (2009). Following the GB/T 1936.1-2009 (2009) and GB1936.2-2009 (2009) standards, the mechanical properties of these woods, including bending strength, bending elastic modulus(MOE), maximum load, and maximum deformation under stress, were studied to conduct compressive experiments using Electromechanical Universal Testing Machine-CMT 6104 with 50-kN load (Sansi, Shenzhen Sansi Zongheng Technology Co., Ltd., China) at a strain rate of 10 mm/min for all samples.

Characterizations

The crystallographic analysis was performed using X-ray diffraction (XRD), a technique that determines atomic arrangements by measuring diffraction angles according to Bragg's law. XRD measurements were conducted on a Rigaku D8 Advance diffractometer (Bruker Corp., Germany) with monochromated Cu K α radiation (λ = 1.5418 Å). The scanning parameters included: 2θ range of 5° to 60°, scan rate of 2°/min, vessel current 40 mA, and accelerating voltage 40 kV.

The XRD patterns revealed patterns expected for wood. Coherent interference produces characteristic peaks in the crystalline regions of wood cellulose, while amorphous domains exhibit diffuse scattering. The crystallinity was calculated as follows:

Cellulose I:
$$CrI = \frac{I_{200} - I_{am}}{I_{200}} \times 100\%$$
 (1)

Cellulose II:
$$CrI = \frac{I_{110} - I_{am}}{I_{110}} \times 100\%$$
 (2)

where CrI is the percentage of relative crystallinity diffraction, I_{200} and I_{110} are extremely diffraction intensities of lattice angle for cellulose I (002) and II (110). I_{am} is the diffraction intensity of the amorphous cellulose (2θ =18° for cellulose I, and 2θ =15° for cellulose II). The number of samples was 5.

To further understand the effects of the hydrothermal-chemical treatments on the bending performance of wood, it is crucial to examine the molecular alterations, particularly in the lignin structure. Fourier-transform infrared spectroscopy (FT-IR), a technique that identifies chemical functional groups through characteristic absorption of infrared radiation, was employed to investigate these chemical changes. The analysis focused on identifying shifts in key functional group absorptions associated with lignin degradation. The changes in the main functional groups were analyzed using an FT-IR spectrometer (Nicolet iN10 MX, USA), with 32 scans per sample acquired in the 4000 to $400 \, \mathrm{cm}^{-1}$ wavenumber range. The mechanical properties were evaluated using a universal testing machine (Shenzhen Sansiwan Co., China).

RESULTS AND DISCUSSION

Microstructure of Wood Samples

The microstructures of the four woods are shown in Fig. 1. Figure 1a shows Yunnan pine (*Pinus yunnanensis*), a coniferous material. Figures 1b, 1c, 1d are hardwood; Fig. 1b is Chinese ash (*Fraxinus chinensis*), a ring-porous material; Fig. 1c is rubberwood (*Hevea brasiliensis*), a porous material; and Fig. 1d is teak (*Tectona grandis*), a semiannular porous material. These anatomical structures and characteristics are shown in Table 2. The microscopic characteristics of the four types of wood are described in Table 3.

The *F. chinensis* wood showed the greatest number of vessels; the *T.* grandis was second; the *H. brasiliensis* vessels showed the fewest, and the *P. yunnanensis* showed no vessels. According to the IAWA broadleaf microscopic characteristics list (IAWA 2004; Schweingruber and Crivellaro 2016), the classification criteria are divided into five grades according to the number of vessels present per square millimeter of wood, with *F. chinensis* and *T. grandis* belonging to grade II (5 to 20 vessels /mm²), and *H. brasiliensis* is grade III.

The diameter of the catheter is divided into four grades according to the classification criteria given by the IAWA broadleaf microscopic characteristics list (2004). *T. grandis* belongs to grade II (50 to 100 μ m), and *F. chinensis* and *H. brasiliensis* belong to grade III (100 to 200 μ m).

The length of wood fiber is divided into three grades according to the classification criteria given by the IAWA broadleaf microscopic characteristics list. *T. grandis*, *F. chinensis*, and *H. brasiliensis* are Grade II (900 to 1600 µm).

The number of wood rays is classified into three grades according to the classification criteria given by the IAWA broadleaf microscopic characteristics list, and *T. grandis*, *F. chinensis*, and *H. brasiliensis* are all Grade II (4 to 12/mm).

The width and height of the wood ray are not graded by IAWA. Therefore, the width of the wood ray is divided into three levels according to the classification criteria of "Wood Science". The width and the fineness are divided into three sublevels. The four woods are all narrow (5 to $100 \, \mu m$). The height of the wood ray is divided into eight grades according to the classification standard of "Wood Science." *T. grandis* and *F. chinensis* are very high (500 to $1000 \, \mu m$), whereas *H. brasiliensis* is high, and *P. yunnanensis* is slightly higher (Shen *et al.* 2020).

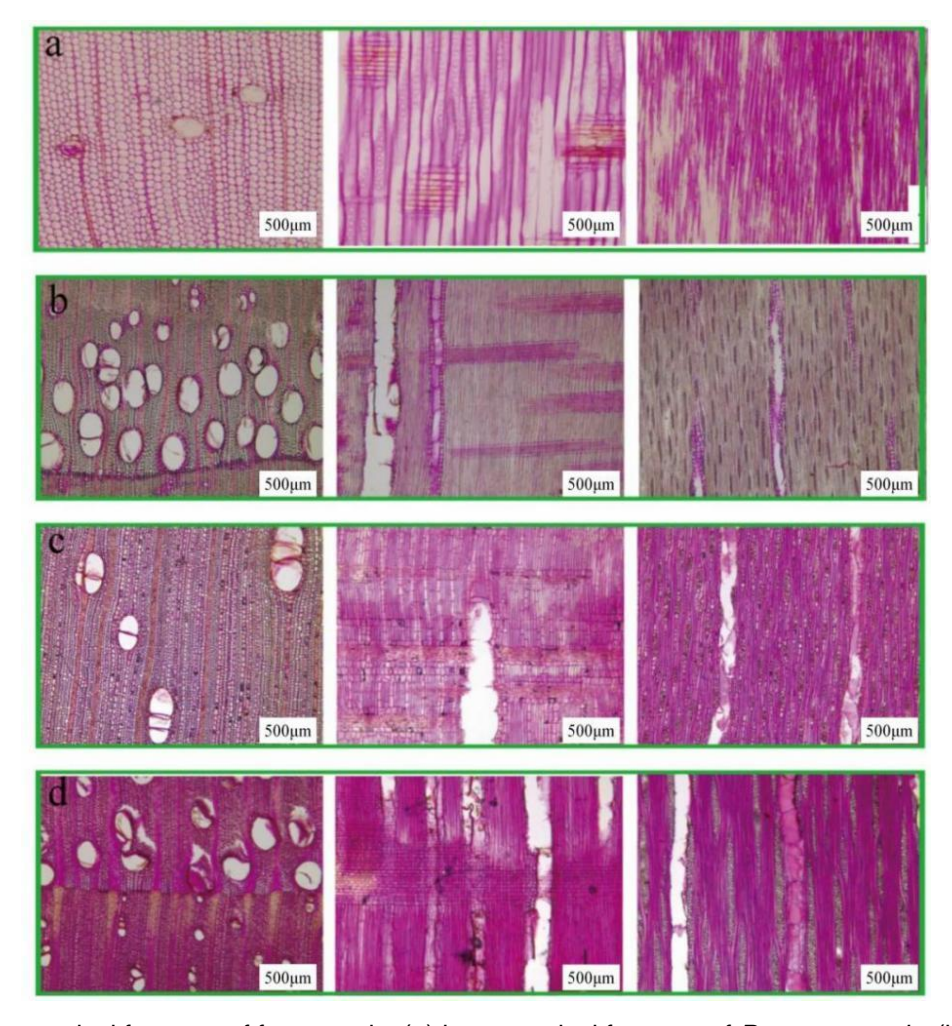


Table 2. Anatomical Structure and Characteristics of Four Kinds of Wood

Anatomical Structure	P.	T.	H.	F.
/ traterribar Stratture	yunnanensis	grandis	brasiliensis	chinensis
Number of vessel (per square millimeter)	N/A	8	3	18
Diameter of vessel (μm)	N/A	87	135	121
Length of vessel (µm)	N/A	287	237	352
Fiber wall thickness (µm)	4.4	8.2	4.7	5.3
Length of fiber (µm)	957	1359	1157	1032
Width of fiber (µm)	40	23	22	21
Number of rays (per square millimeter)	5	6	9	11
Height of uniseriate rays (cells)	1-20	1-6	1-12	1-10
Width of uniseriate rays (cells)	1	1	1	1
Height of multiseriate rays (cells)	1-10	4-63	4-20	4-30
Width of multiseriate rays (cells)	2-3	2-5	2-4	2-4

Table 3. Microscopic Features of Four Types of Wood

Varieties of Trees	Microscopic Characteristics of Four Types of Wood
F. chinensis	The wood vessels are ovoid in shape in the early wood zone cross-section, with simple pores and short radial compound pores, scattered or obliquely arranged. No tyloses are observed. Thread thickening is absent. Simple perforation, with perforation plates slightly inclined. Interlocking pits between vessels. Axial parenchyma rings are tubular, ring-shaped, and a few wing-shaped, as well as ring-shaped; parenchyma cells are clearly thickened in nodes, without resin crystals observed. Wood fibers usually have thin walls, narrow pits, and few in number. Wood rays are not superimposed, with a few simple rays, 1-10 cells high; multiple rays are 2-4 rows wide and 4-30 cells high; ray tissue is either simple or multiple rows, with round or ovoid ray cells; contains a small amount of resin, no crystals observed, end wall thickening and horizontal wall pits are obvious; ray-vessel interlocking pits are similar to interlocking pits between vessels.
T. grandis	The wood vessels are ovoid and round in early wood cross-sections, with simple pores and short radial rows of compound pores, scattered or several in an oblique row, with tyloses. Thread thickening is absent. Simple perforations, round and ovoid to elliptical, with perforation plates parallel and slightly inclined, interlocking pits between vessels, ovoid. Axial parenchyma is ring-shaped or straight ring-like bundles, with obvious node-like thickening at the end walls of the parenchyma, containing a small amount of gum, no crystals observed. Wood fibers have thin walls, slightly obvious bordered pits, and are round. Wood rays are not superimposed, with very few simple rays, 1-6 cells high; multiple rays are 2-5 cells wide and 4-72 cells high, with occasional double rows of multiple rays within the same ray; ray tissues are simple and multiple rows, rarely irregular type III; ray cells are elliptical and ovoid, containing gum, no crystals observed; node-like thickening at the end walls and horizontal wall pits are obvious; the pattern of pits between rays and vessels is similar to that between vessels.
H. brasiliensis	The wood vessel is ovoid in shape in the early wood zone cross-section, with 2-4 short-diameter rows of compound pores, sparsely to clustered pores, no tyloses observed, and absent thread thickening. Single perforation, with slightly inclined perforation plate. Interlocking pits between vessels. There is a large amount of axial parenchyma, mainly in the form of discrete vessel bands, ring-shaped vessels, ring-shaped vessel bundles, and a few scattered; no gum is contained, and diamond crystals are occasionally seen. The wood fiber wall is thin, with many marginal pits, slightly obvious, and round. The wood rays are not superimposed, with single-row rays ranging from 1-12 cells, multiple rows of 2-4 cells wide, and 4-31 cells high; ray tissue heterogeneity types I and II. Ray cells usually do not contain gum, saw diamond crystals, and the interlocking pits between rays and vessels are similar to those between vessels.
P. yunnanensis	The cross-section of early wood tracheids is polygonal and rectangular; the radial wall pits are 1-2 rows, oval and round. The axial parenchyma is absent. There are single-row and spindle-shaped wood rays: the single-row rays are 1-20 cells high, and the spindle-shaped wood rays have radial resin vessels, 1-10 cells high; ray tracheids exist in both types of cells, located in 1-4 rows on the upper and lower edges. The inner wall is deeply serrated, and the outer edge is wavy. The horizontal walls of the ray parenchyma cells are thin, with few pits, no end wall node thickening, and few indentations. The pattern of pits between ray parenchyma cells and early wood tracheids is fenestrated, usually 1-3.

Chemical Composition of Wood Samples

Four types of wood softening pretreatment

The wood was sawn into a 300 mm \times 20 mm \times 20 mm specimen, and a sander was used to smooth the surface of the wood. Specimens were placed in a convection drying oven at 103 °C until it was completely dry. After cooling, the wood was weighed. A laser engraver was used to engrave the specimen number corresponding to the weight. The prepared specimens were immersed in water, ammonia, and a compound alkali solution until the moisture content was approximately 40%. The impregnated specimens were wrapped with plastic wrap and placed in a vertical pressure steam sterilizer (BOXUN, Shanghai Boxun Industrial Co., Ltd.) for steam softening treatment, with a set temperature of 110 °C and a treatment time of 6 h.

XRD analysis

The XRD test results of the four woods are shown (Fig. 2). For the four woods, hydrothermal treatment, ammonia treatment, and compound lye treatment all increased the relative crystallinity of the wood. The order of increase in relative crystallinity was hydrothermal treatment < ammonia treatment < complex lye treatment. Among this progression in crystallinity, the increase in the F. chinensis was not large but was gradual and showed the greatest increase when F. chinensis was treated with lye. The increase in the H. brasiliensis was very large, and the difference between the results of the ammonia treatment and compound lye treatment was not great and was greatest with the lye treatment. The crystallinity of the *T. grandis* treatment increased greatly, with the increase after treatment being even, and the increase after treatment with the lye compound being the largest. The crystallinity of the P. yunnanensis increased greatly, but the change in softening was not as great with the lye treatment.

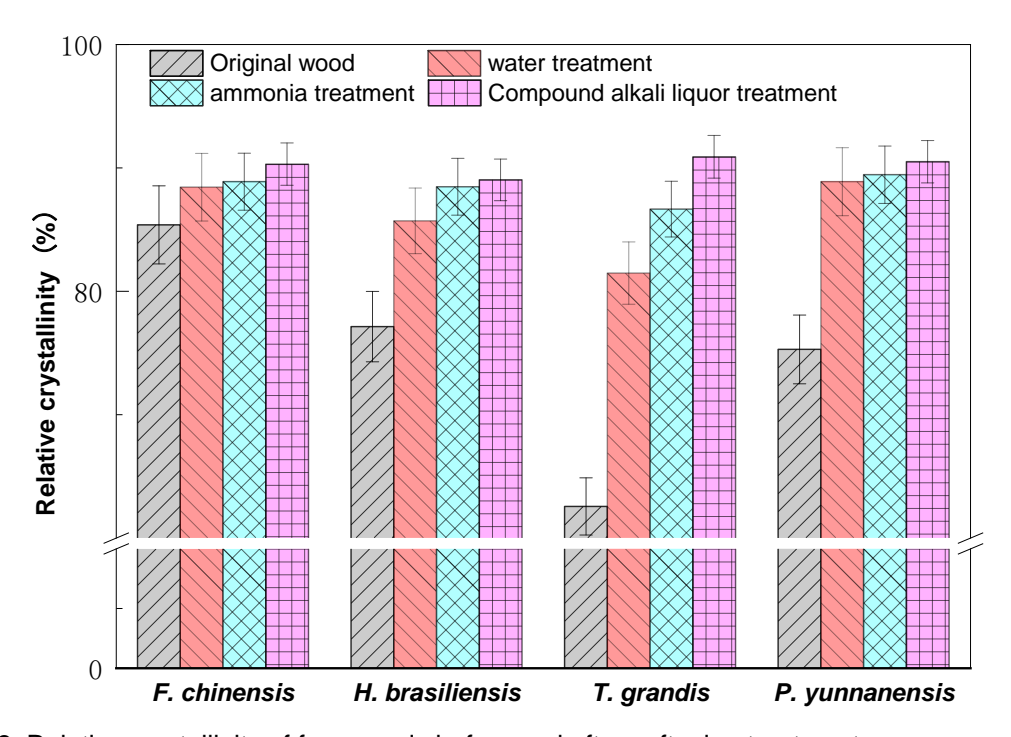


Fig. 2. Relative crystallinity of four woods before and after softening treatment

4644

As shown in Fig. 2, the XRD patterns of the hydrothermal treatment, the ammonia treatment, and the lye compound treatment samples were compared with the XRD images of the four wood material samples (Fig. 3), and the positions of the 101 and 002 diffraction peaks were 16° and 22.5°, respectively. This result shows that the hydrothermal treatment, ammonia treatment and compound lye treatment had no effect on the crystallization zone of the wood sample; that is, the crystal layer distance does not change.

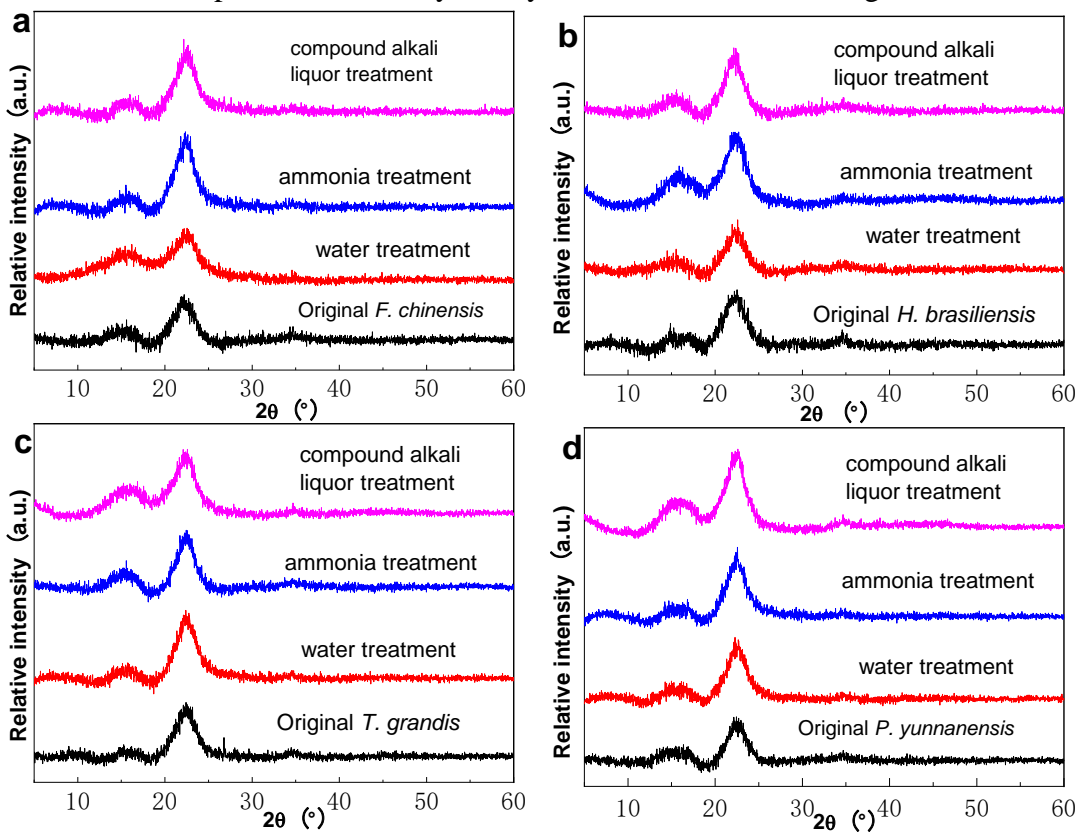


Fig. 3. XRD patterns of four woods. (a) is XRD patterns of *F. chinensis*; (b) is XRD patterns of *H. brasiliensis*; (c) is XRD patterns of *T. grandis*; (d) is XRD patterns of *P. yunnanensis*

The order of effects on crystallinity of the four kinds of wood material was as follows: wood material < water treatment < ammonia treatment < compound lye treatment: that is, the relative crystallinity of the sample is increased after the treatment with the compound lye, mainly because of the alkali compound. The liquid enters the monocrystalline zone of the cellulose, hemicellulose and lignin in the wood, causing it to degrade, whereas the hydrothermal treatment, the ammonia treatment and the compounding alkali treatment processes extract the water from the amorphous zone in the wood. The surface of the cellulose microfibril has hydroxyl groups, and the microfibrils in the amorphous region tend to be stable and increase the relative crystallinity; that is, the compound alkali solution may enter the crystallization zone of the wood, and the ammonia water volatilizes and crystallizes in the compound alkali solution. The influence on the crystallization zone is small, so the relative crystallinity is increased. A difference was observed in the relative crystallinity of the four woods. The main reason is the difference in the hydrothermal degradation of the wood caused by the different contents of lignin, cellulose, and hemicellulose in the four wood samples. The difference in the amount of extractables in the wood resulted in a large difference in the extent of the relative

crystallinity of the wood samples after hydrothermal treatment, ammonia treatment, and compound lye treatment (Sun and Li 2010).

FT-IR analysis

The main characteristics of the infrared spectrum of the four kinds of wood treated by the compounding lye softening modification are as shown in Table 4.

 Table 4. FT-IR Absorption Bands in Wood Treated with CAL Softening

Range of Wavenumbers (cm ⁻¹)	Absorption Band Attribution and Description
3412 to 3460	O-H stretching vibration
3000 to 2845	C-H stretching vibration (CH ₃ , CH ₂)
1736 to 1709	C=O stretching vibration (Acetyl in xylan)
1675 to 1655	C=O stretching vibration (Conjugated aryl ketone in lignin)
1605 to 1593	C=O stretching vibration and aromatic skeleton vibration (Lignin)
1515 to 1505	Benzene ring skeleton vibration (Lignin)
1470 to 1460	C-H Bending vibration (Lignin), asymmetric bending vibration of CH ₃ and CH ₂
1430 to 1422	C-H Bending vibration (Lignin, CH ₂ in glycans), benzene ring skeleton vibration (Lignin)
1370 to 1365	C-H Bending vibration (Cellulose, Hemicellulose)
1330 to 1328	C-H Bending vibration (Cellulose, Lilac based and guaiac wood condensation, Lilac-based C-O vibration
1230 to 1221	Ar-O stretching vibration in benzene ring (Lignin), Pyranose C-O-C stretching vibration
1157	C-O-C stretching vibration (Cellulose, Hemicellulose)
1058	C-O stretching vibration (Cellulose, Hemicellulose)
1038 to 1025	In-plane bending vibration of C-H benzene ring
897	Cellulose β chain characteristics

Figure 4 shows the FTIR spectra of the *F. chinensis*, *H. brasillensis*, *T. grandis*, and *P. yunnanensis* materials, control groups (*i.e.*, the raw materials), and the hydrothermal treatment, ammonia treatment, and compound lye treatment. Four wood materials and water are shown.

For the four wood samples subjected to hydrothermal treatment, there was no significant change or weakening in the absorbance peaks of the spectra compared to the control group. Therefore, the four types of wood samples subjected to hydrothermal treatment did not have a significant impact on their chemical composition.

The four samples treated with ammonia showed a decrease in the three absorbance peaks at 1736, 1594, and 1227 cm⁻¹ for *F. chinensis* wood and *T. grandis*. The absorbance peak at 1736 cm⁻¹ is mainly due to the stretching vibration of acetyl C=O in wood, the absorbance peak at 1594 cm⁻¹ is mainly due to the vibration of the phenyl carbon skeleton and the stretching vibration of C=O, and the absorbance peak at 1227 cm⁻¹ is mainly due to the stretching vibration of C-O-C in pyranose. The absorbance peaks of *H. brasiliensis* at 2900, 1736, 1510, and 1240 cm⁻¹ were weakened. The absorbance peak at 2900 cm⁻¹ is mainly due to the asymmetric deformation of methyl groups, lignin, and -CH₂ in polysaccharides. The increase in these two absorbance peaks indicates that the molecular structure of lignin has changed due to the compound alkali solution. The three absorbance peaks of ammonia-treated *P. yunnanensis* at 1636, 1460, and 1425 cm⁻¹ were weakened. The absorbance peak at 1636 cm⁻¹ is mainly due to the stretching vibration of C=O, and the absorbance peak at 1460 cm⁻¹ is mainly due to the asymmetric deformation of methyl

groups, lignin, and -CH₂ in polysaccharides. In summary, ammonia treatment changes the molecular structure of lignin and hemicellulose in the four types of wood, and under the action of temperature and ammonia; there is a certain degree of degradation in *F. chinensis* wood samples (Wang *et al.* 2019).

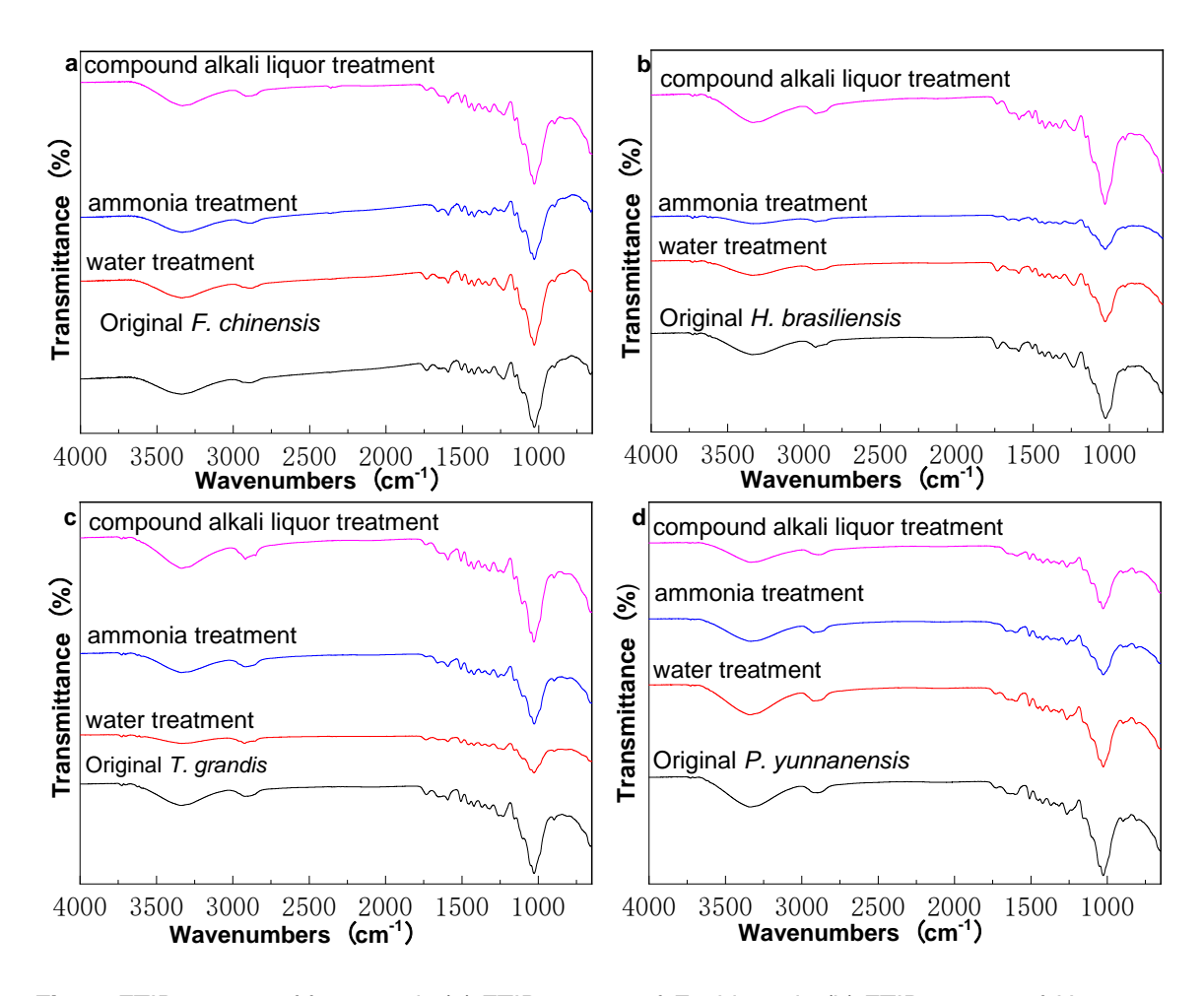


Fig. 4. FTIR spectra of four woods (a) FTIR spectra of *F. chinensis*, (b) FTIR spectra of *H. brasiliensis*, (c) FTIR spectra of *T. grandis*, and (d) FTIR spectra of *P. yunnanensis*

After treatment with the composite alkali solution, all four different wood samples exhibited corresponding changes in characteristic peaks. For *F. chinensis* wood, six absorbance peaks appeared at 3417, 2900, 1460, 1400, 1066, and 800 cm⁻¹, all of which underwent varying degrees of change. The absorbance peak at 3417 cm⁻¹ is primarily due to the stretching and vibration of O-H bonds on the wood surface, indicating that the composite alkali solution treatment allows the wood surface to adsorb more water molecules, resulting in the presence of more hydroxyl groups. The absorbance peaks at 2900 and 1460 cm⁻¹ were enhanced. The absorbance peak at 2900 cm⁻¹ is mainly due to the stretching and vibration of C-H bonds in methyl and methylene groups on the wood surface, while the absorbance peak at 1460 cm⁻¹ is primarily due to the asymmetric stretching and vibration of methyl groups and the deformation vibration of -CH₂ bonds in lignin and polysaccharides. The enhancement of these two absorbance peaks indicates that the composite alkali solution had caused changes in the molecular structure of lignin. Additionally, the absorbance peaks at 1400, 1066, and 800 cm⁻¹ were also enhanced. The

absorbance peak at $1400 \, \mathrm{cm^{-1}}$ is mainly due to the deformation and stretching vibration of C-H bonds in the benzene ring skeleton, the absorbance peak at $1066 \, \mathrm{cm^{-1}}$ is primarily due to the stretching vibration of C-O bonds in pyranose, and the absorbance peak at $800 \, \mathrm{cm^{-1}}$ is mainly due to the characteristic vibration of β -chains in cellulose. From this, it can be concluded that the composite alkali solution had caused a certain degree of degradation in the molecular structures of lignin, cellulose, and hemicellulose, allowing the wood to adsorb more water molecules, increasing the distance between molecular chains, significantly reducing the binding strength between molecules, and lowering the physical and mechanical properties of F. chinensis wood, which is beneficial for bending F. chinensis wood.

For *H. brasiliensis* treated with a compound alkali solution, six absorbance peaks changed at 3421, 2900, 1430, 1266, 1227, and 897 cm⁻¹. After treatment with the compound alkali solution, *P. yunnanensis* showed six absorbance peaks at 3331, 2900, 1659, 1594, 1225, and 835 cm⁻¹, all of which changed to varying degrees. *T. grandis* softened with the compound alkali solution showed seven absorbance peaks at 3417, 1736, 1658, 1594, 1266, 1227, and 897 cm⁻¹, all of which changed to varying degrees. The reasons for the changes in the absorption peak values of *H. brasiliensis*, *P. yunnanensis*, and *T. grandis* are generally similar to those of white wax wood. It can be inferred that the compound alkali solution degrades the molecular structures of lignin, cellulose, and hemicellulose to a certain extent, allowing the wood to adsorb more water molecules, increasing the distance between molecular chains, reducing the binding strength between molecules, and significantly reducing the physical and mechanical properties of the four different wood samples, which is beneficial for wood bending.

In summary, these shifts point to selective lignin degradation during chemical treatment, which alters the wood's microstructure, making the fibers more pliable and affecting the bending properties. Thus, FT-IR analysis not only confirms the chemical treatment's efficacy but also provides a molecular-level understanding of how selective lignin degradation facilitates improved bending deformation and workability in treated wood samples. The overall difference in absorption intensity after heat treatment and ammonia treatment was not significant. The increasing order was complex lye treatment > material > hydrothermal treatment > ammonia treatment; the use of composite alkali solution treatment greatly improves the absorption intensity.

Physical and Mechanical Properties

Moisture content and density

The statistical analysis results of the air-dried density, oven-dried density, and basic density of the four types of wood are shown in Table 5. The basic densities of F. chinensis, T. grandis, H. brasiliensis, and P. yunnanensis were 0.54, 0.65, 0.65, and 0.52 g/cm³, respectively. The air-dried densities were 0.70, 0.70, 0.68, and 0.62 g/cm³, respectively. According to the classification of air-dried density for Chinese timber, all four wood species are classified as medium density. The variance analysis of the density differences between the four species shows that the basic density, air-dried density, and full-dry density all differed significantly (P < 0.01). Significant differences were found between F. chinensis, T. grandis, H. brasiliensis, and P. yunnanensis. This indicates that the density differences among the four wood species were statistically significant.

Furthermore, based on the significance results of analysis of variance, Tukey's HSD (Least Significant Difference) test was used to compare the density differences between different woods. The results of Tukey's HSD test are shown in Table 6.

Based on the analysis results of ANOVA and Tukey's HSD test, the following conclusions can be drawn: The densities of the four wood species showed significant differences in terms of basic density, air-dry density, and oven-dry density (all P-values were less than 0.05). Specifically, significant density differences were found between *F. chinensis* and *T. grandis*, *F. chinensis* and *H. brasiliensis*, *T. grandis* and *P. yunnanensis*, and *H. brasiliensis* and *P. yunnanensis*, while no significant density difference was observed between *F. chinensis* and *P. yunnanensis*, and between *T. grandis* and *H. brasiliensis*. These density differences provide valuable insights for further studies on the mechanical properties of wood (such as bending strength and modulus of elasticity), suggesting that the density differences among different wood species may significantly affect the mechanical properties of wood.

Comparative analysis of dimensional stability

According to the experimental results, the average values of the shrinkage and swelling coefficients taken from a radial direction and chordwise and the volume of the four woods in the three states of air drying, dryness and saturated wet expansion are shown in Table 7. In all three states, for the four types of wood, the radial coefficients were less than those of the chord, whether the wood is dry or not. Under the three different environmental humidities, the average wood radial air dry shrinkage values, total dry shrinkage and saturated wet expansion of the four types of wood were less than 1.5% according to the grading standards given by WG KEATING for the four wood gases. The dry shrinkage, the total dry shrinkage ratio, and the saturated wet expansion ratio were all small. As a result, the four types of wood have good dimensional stability and are not easily deformed.

Effect of weight gain rate on wood bending performance

Figure 5 shows the physicomechanical properties and bending properties of the three kinds of wood samples. The damage load, bending strength, and elastic modulus of the four woods were the highest, respectively, at 2570 N, 116 MPa, and 10600 MPa, followed by *P. yunnanensis* and then *T. grandis*, with *H. brasiliensis* showing the lowest values, namely, 1940 N, 88 MPa, and 8340 MPa. *F. chinensis* showed the largest bending deformation, with an average h/r of 0.03, with the others showing a value of 0.02.

 Table 5. Statistics and Variance Analysis on Four Wood Species Density

		Ana	lysis of Varia	ance	Statistical Analysis				
Tree Species	Parameter	mean square	F	Р	Mean	Standard Deviation	Standard Error	Coefficient of Variation	
	Basic density	5.1564	7.85	0.0019	0.54	0.016	0.005	2.99	
F. chinensis	Air dry density	5.1565	7.34	0.0026	0.70	0.019	0.006	2.75	
	Full dry density	5.1565	7.45	0.0024	0.66	0.021	0.007	3.16	
	Basic density	5.1567	7.81	0.0019	0.65	0.028	0.009	5.07	
T. grandis	Air dry density	5.1577	8.06	0.0017	0.70	0.047	0.016	9.99	
	Full dry density	5.1565	7.93	0.0018	0.66	0.021	0.007	4.08	
	Basic density	5.1565	7.88	0.0019	0.65	0.019	0.006	3.72	
H. brasiliensis	Air dry density	5.1567	7.51	0.0023	0.68	0.026	0.008	4.06	
	Full dry density	5.1566	7.66	0.0021	0.63	0.025	0.008	4.20	
P. yunnanensis	Basic density	5.1552	7.59	0.0017	0.52	0.017	0.005	8.37	
	Air dry density	5.1572	7.84	0.0016	0.62	0.043	0.007	5.21	
	Full dry density	5.1563	7.77	0.0020	0.27	0.026	0.006	5.77	

Table 6. The Results of Tukey's HSD Test

Comparison	Mean Difference	Standard Error	Р	Significance
F. chinensis vs T. grandis	-0.11	0.030	0.008	Significant
F. chinensis vs H. brasiliensis	-0.10	0.028	0.015	Significant
F. chinensis vs P. yunnanensis	0.02	0.029	0.890	No Significant Difference
T. grandis vs H. brasiliensis	0.01	0.032	0.947	No Significant Difference
T. grandis vs P. yunnanensis	0.13	0.031	0.002	Significant
H. brasiliensis vs P. yunnanensis	0.14	0.030	0.001	Significant

Table 7. Dry Shrinkage and Swelling Characteristics of Four Kinds of Wood

Sample	Air-Dry Shrinkage Rate (%)			Absolute Dry Shrinkage Rate (%)			Saturated Swelling Rate (%)		
Direction	Radial	Tangential	Volume	Radial	Tangential	Volume	Radial	Tangential	Volume
F. chinensis	0.24	0.57	0.82	0.38	0.77	1.04	0.57	0.74	1.23
H. brasiliensis	0.21	0.36	0.67	0.36	0.68	0.97	0.69	0.80	1.37
T. grandis	0.34	0.49	0.77	0.46	0.97	1.24	0.56	0.87	1.32
P. yunnanensis	0.21	0.35	0.61	0.35	0.68	1.07	0.61	0.87	1.44

In the three kinds of wood samples treated with three solutions under different weight gain conditions, the breaking load, static bending strength and elastic modulus decreased with the increase in water content. The magnitudes of failure load, static bending strength and elastic modulus were as follows: material >> water treatment sample > ammonia treatment sample > complex lye treatment sample. The trend of four wood samples failure was F. chinensis > H. brasiliensis > T. grandis > P. yunnanensis. Figure 5d shows the effect of weight gain rate on the bending properties of the four wood samples treated with three solutions. As can be seen from the figure, the bending performance and weight gain rate of the three solution-treated woods were high in the middle and low on both sides. The weight gain of the three solutions increased before 40% and then gradually decreased. The h/r values of F. chinensis, H. brasiliensis, T. grandis, and P. yunnanensis after water treatment were 40%; the values of the bending performance were 0.065, 0.049, 0.058, and 0.069, respectively; the values for the ammonia treatment were 0.079, 0.081, 0.057, and 0.069, respectively; and the values with the compound lye treatment were 0.096, 0.102, 0.075, and 0.074, respectively. For the three solutions, the flexural performance of the sample treated with compound lye > the bending performance of the sample treated with ammonia solution > the worst bending performance of the sample treated with hydrothermal treatment. But the wood samples for the species did bend with the hydrothermal treatment. The difference in performance was small, but the lye and ammonia treatments showed higher bending properties of the material.

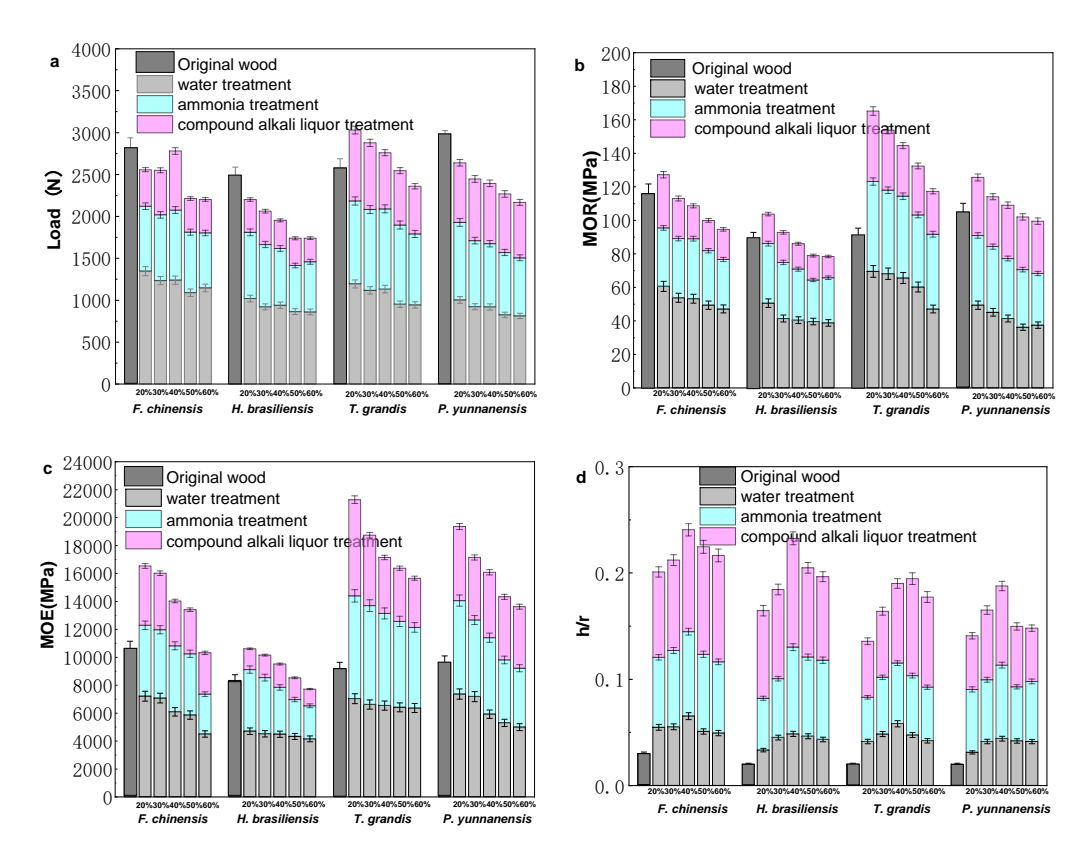


Fig. 5. Effect of weight gain rate of three reagents on physical and mechanical properties and bending properties of four wood samples.(a) is the effect of the failure load of the wood sample; (b) is the effect of the flexural strength of the wood specimen; (c) is the effect of the modulus of elasticity of the wood sample; (d) is the effect of the bending properties of the wood specimen.

In the ammonia-treated sample, the bending performance of F. chinensis and H. brasiliensis was significantly > T. grandis and H. brasiliensis; as for the sample treated with compound lye, the bending performances of the H. brasiliensis > F. chinensis > T. grandi > P. yunnanensis. Therefore, the bending property of the wood was not only related to the change of the weight gain rate but was also related to softener, with the tree species being the biggest factor when determining the bending property of the wood.

Figure 6 illustrates the physical, mechanical, and bending properties of the four wood species. When treated with three softening agents under varying temperature conditions, the breaking load, static bending strength, and elastic modulus of all wood samples decreased progressively with increasing hydrothermal treatment temperature. Additionally, the samples exhibited brittle fracture behavior at elevated temperatures, indicating a loss of structural integrity under thermal stress. The static bending strength and the elastic modulus were the material >> water treatment sample > ammonia treatment sample > complex lye treatment sample. The trend of the four wood samples to fail was F. chinensis > H. brasiliensis > T. grandis > P. yunnanensis. Figure 6d shows the effect of the hydrothermal treatment temperature on the bending properties of the four wood samples treated with the three solutions. As shown, the bending performance and weight gain of the three solutions used on the treated wood were high in the middle and low on both sides. After the three softener treatments had been applied and when the treatment temperature was between 90 and 120 °C, the four woods showed the highest bending performance (at 120 °C), except for F. chinensis.

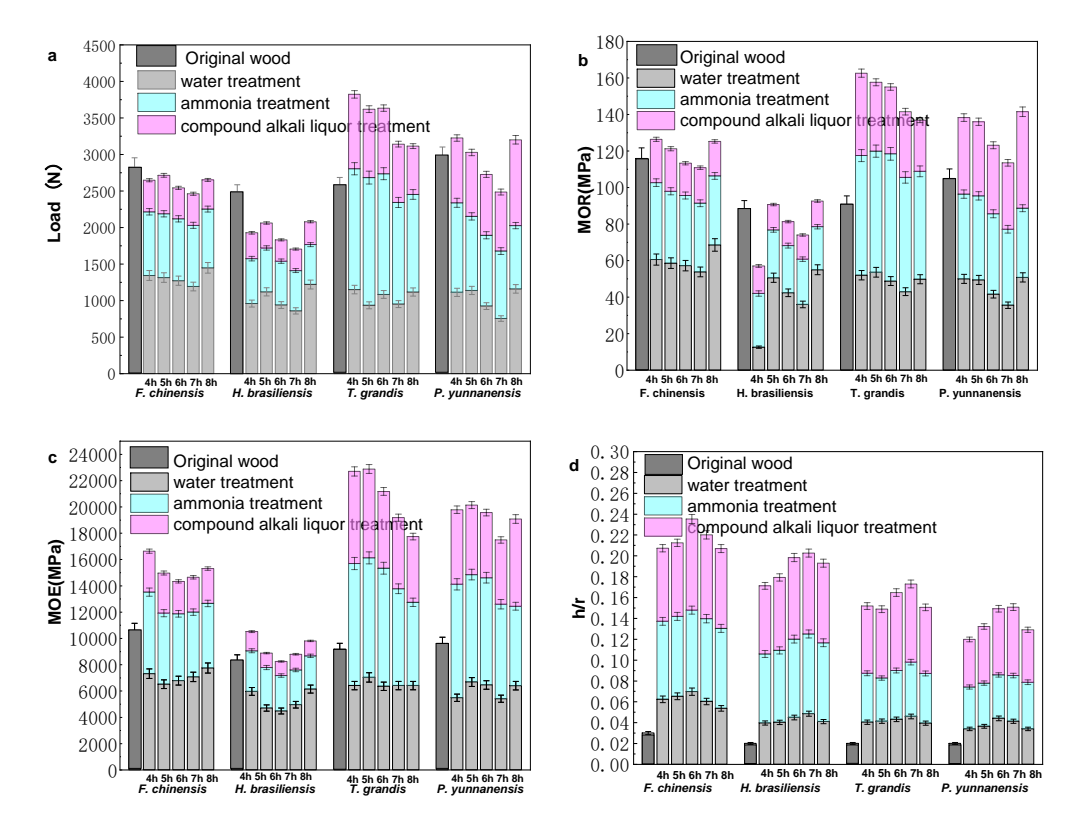


Fig. 6. Effect of hydrothermal temperature of three reagents on physical and mechanical properties and bending properties of four wood specimens.(a) is the effect of the failure load of the wood sample; (b) is the effect of the flexural strength of the wood specimen; (c) is the effect of the modulus of elasticity of the wood sample; (d) is the effect of the bending properties of the wood specimen

When the temperature exceeded 120 °C, the wood bending properties decreased with increasing temperature. The h/r values of *F. chinensis*, *H. brasiliensis*, *T. grandis*, and *P. yunnanensis*, after water treatment and when the hydrothermal temperature was 120 °C, were 0.060, 0.049, 0.046, and 0.041, respectively; after ammonia treatment, 0.079, 0.076, 0.052, and 0.044, respectively; and after complex lye treatment, 0.080, 0.078, 0.075, and 0.066, respectively. The bending performance enhancements followed: compound lye treatment > ammonia treatment > hydrothermal treatment, despite minor inter-treatment differences (Fig. 2). Species-specific rankings under each solution were: Ammonia-treated samples: *F. chinensis* > *H. brasiliensis* > *T. grandis* > *P. yunnanensis*. Notably, *H. brasiliensis* exhibited reversed efficacy between treatments (ammonia > lye), suggesting softener chemistry (e.g., lignin plasticization) and species-specific anatomy (vessel density: *F. chinensis* > *H. brasiliensis* > *T. grandis* > *P. yunnanensis*) jointly govern bending outcomes, consistent with Fig. 2.

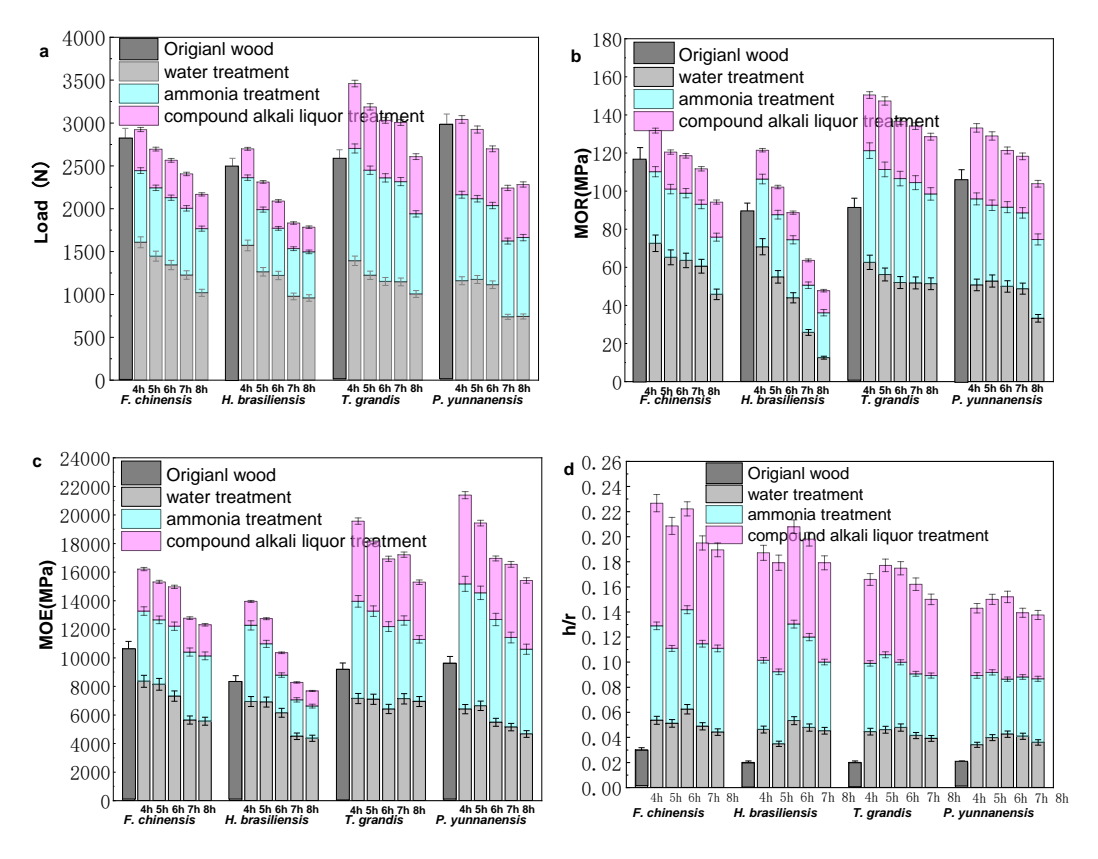


Fig. 7. Effect of hydrothermal time of three reagents on physical and mechanical properties and bending properties of four wood specimens: (a) is the effect of the failure load of the wood sample; (b) is the effect of the flexural strength of the wood specimen; (c) is the effect of the modulus of elasticity of the wood sample; (d) is the effect of the bending properties of the wood specimen

Figure 7 shows the physical and mechanical properties and bending properties of the four wood samples. In the four kinds of wood samples treated with three kinds of solutions under different processing times, the breaking load, static bending strength, and elastic modulus decreased with the increased in the hydrothermal treatment temperature,

until damaged. The load, static bending strength and elastic modulus were greatest according to the order of material >> water treatment sample > ammonia treatment sample > complex lye treatment sample, and the trend in the failure of the four wood samples was F. chinensis > H. brasiliensis > T. grandis > P. yunnanensis.

Figure 7d shows the effect of hydrothermal treatment time on the bending properties of the four wood samples treated with three kinds of solutions. The bending performance and weight gain of the three solution-treated woods were high and low on both sides. When the time was between 4 and 6 h, the bending performance showed an upward trend. With the three softener treatments, the four woods had the highest bending performance at 6 h of treatment, but when the treatment time exceeded 6 h, the wood bending properties all decreased with time. The h/r values of *F. chinensis*, *H. brasiliensis*, *T. grandis* and *P. yunnanensis* after water treatment were 0.062, 0.053, 0.048, and 0.043 when the hydrothermal temperature was 120 °C; 0.079, 0.077, 0.052, and 0.044 for the ammonia treatment; and 0.098, 0.087, 0.075, and 0.067 for the complex lye treatment. Among the three solutions, the wood sample treated with the lye treatment solution ranked first in bending performance, the ammonia solution treatment sample was second, and the hydrothermal treatment sample ranked third.

For the hydrothermal treatment time, the bending performance of the tested piece differed little with the change in hydrothermal time, but the treatment increased the bending property of the material. However, the ammonia-treated sample ranked first in bending performance, while the water-treated test piece ranked second. Among samples treated with the compound alkali solution, *F. chinensis* wood ranked first, *H. brasiliensis* second, *T. grandis* third, and *P. yunnanensis* ranked fourth. Therefore, the bending property of the wood is not only related to the hydrothermal treatment time but is also related to the softener, with the tree species being the biggest factor determining the bending property of the wood, a finding consistent with the conclusions of Figs. 2 and 3.

According to the above results, the change of wood moisture content greatly influenced the mechanical properties of the wood. When the water content was below the fiber saturation point, the strength of the wood decreased with the increase of moisture in the wood, mainly due to the unit volume. The binding force between the inner cellulose and the lignin molecule is increased when the water content is above the fiber saturation point, and as the free water content is continuously increased, the wood strength remains substantially unchanged or decreased. However, water is a plasticizer that can enter the amorphous zone of wood, causing the amorphous zone to swell and depolymerize a portion of cellulose, hemicellulose, and lignin under temperature, and with water content. This increase in water will also decrease the glass transition temperature of the wood, so the elastic modulus of the wood will gradually begin to decrease with the increased in the weight gain rate. This occurs because free water will appear in the cell cavity, and free water will begin the process of bending the wood. The stress is generated to hinder the bending of the wood so that, when the water content is too high, the bending property is lowered. Ammonia water can enter the amorphous zone of wood to produce ammoniated cellulose, which causes the wood to further swell. At the same time, ammonia can degrade some lignin, which will improve the bending property of the wood and reduce the elastic modulus of the wood. However, excessive treatment of ammonia will reduce the strength and lead to a decrease in the bending properties of the wood. The content of ammonia in the compound lye is lower than that of ammonia water, which will reduce the influence of the decrease in the strength of the wood during the treatment. At the same time, the compound lye contains additives such as lubricants and swelling agents to influence the

wood fiber in the bending process, making it easier to stretch but not tear the fibers. The results show that the compound lye was able to obtain higher h/r values than water and ammonia.

The influence of hydrothermal temperature on the mechanical properties of wood was more complicated; that is, the influence was small at room temperature, whereas high temperature and extreme low temperature were found to have great influence. If the temperature is too high, the moisture content of the wood and its distribution will be uneven, which causes stress, drying and carbonization in the wood. These effects occur mainly because the temperature promotes the vigorous movement of the cell wall material molecules, the internal friction is reduced, and the microfibrils are loose; that is, when the wood is at a high temperature, the hydroxyl groups on the surface of the cellulose and hemicellulose are reduced, the hemicellulose is degraded, and the wood gradually carbonizes. The brittleness is increased, and the strength is lowered. For most woods, however, the mechanical properties decrease with increasing hydrothermal treatment temperatures. Different tree species have great differences in vessel distribution and fiber ratio, length and angle, which lead to great differences in the temperature change of wood during hydrothermal treatment, but the overall trend is the same; that is, the temperature rises and decreases, but exceeding a certain temperature causes the wood components to be destroyed and affects the bending properties of the wood.

The degradation of cellulose and hemicellulose becomes significant at elevated temperatures. Under long-term hydrothermal treatment (approximately 83 °C), extractives, pectin, and hemicellulose in wood are partially or completely dissolved or hydrolyzed into soluble low-molecular-weight substances (*e.g.*, monosaccharides and organic acids). This loss of structural components weakens the wood matrix, leading to reduced bending properties. Notably, the effects of prolonged high-temperature hydrothermal treatment on wood properties are cumulative, as progressive removal of hemicellulose and amorphous polymers further compromises mechanical strength. For most woods, however, the mechanical properties decrease with increasing hydrothermal treatment time. Different tree species have great differences in vessel distribution and fiber ratio, length and fiber angle, which lead to great differences in the treatment time of wood during hydrothermal treatment, but the overall trend is the same. That is, the increase in time is reduced, but after a certain period of time, the wood component is depolymerized, and the bending property of the wood is affected.

At the same time, for tree species, the composition of hardwood and softwood is very different, with broadleaf trees showing a very different vessel distribution and fiber ratio, length and fiber angle, which contribute to the physical and mechanical properties of the wood. Therefore, differences exist in the optimum weight gain rate and the softening effect of the different softeners in the softening process of wood.

Correlation Analysis

The Pearson correlation coefficients between the maximum bending deformation of wood and anatomical features, as well as physical and mechanical property parameters, are shown in Table 8.

Table 8. Correlation Analysis Bending Deformation Quantity and Anatomical
Parameters, and Physical-Mechanical Performance of Six Wood Species

Index	Maximum Deformation	Maximum Load	Elastic Modulus	Bending Strength	Conduit Ratio	Fiber Length	Density
Maximum deformation	1	0.566	0.371	0.566	0.832	0.563	-0.510
Maximum load		1	0.357	0.300	0.833	0.581	0.562
Elastic modulus			1	0.257	-0.819	0.533	0.556
Flexural strength				1	0.833	0.581	0.562
Vessel ratio					1	0.558	-0.513
Fiber length						1	0.507
Density							1

The ratio of vessels was highly correlated with the amount of bending deformation in wood; fiber length and maximum load were moderately correlated with the amount of bending deformation in wood; density was moderately negatively correlated with the amount of bending deformation in wood; while bending strength and elastic modulus were weakly correlated with the amount of bending deformation in wood. Through a comprehensive evaluation of the anatomical characteristics and physical and mechanical properties of wood, F. chinensis wood is characterized by straight grain, good dimensional stability, moderate to slightly above average static bending strength, elastic modulus, and load strength; its vessel ratio and wood fiber length are both moderately above average, and its density is low, which promotes bending deformation in wood. The extent of bending of F. chinensis wood was significantly greater than the other three species of wood. Therefore, F. chinensis wood was found to be the easiest to bend, while T. grandis was the most difficult to bend. This is due to the significant differences in the internal structure of different species of wood, which results in significant differences in bending performance. The size of vessels and the length of wood fibers in broadleaf trees are beneficial to the bending of wood, while density inhibits the bending performance of wood. Therefore, selecting the appropriate species of wood is beneficial for the production of bent wood.

Discussion

The primary objective of this study was to investigate the bending performance of four types of wood (*F. chinensis*, *T. grandis*, *H. brasiliensis*, and *P. yunnanensis*) under different softening treatments, including water treatment, ammonia treatment, and composite alkali treatment. The findings from the three-point bending tests and subsequent analyses of physical and mechanical properties provide valuable insights into the relationship between wood species, softening treatments, and bending performance.

Influence of wood species on bending performance

The results of this study revealed that different wood species exhibited significant variations in bending performance, with notable differences in bending strength and elastic modulus. Specifically, *T. grandis* and *H. brasiliensis* demonstrated higher bending strength compared to *F. chinensis* and *P. yunnanensis*. These differences are likely attributable to the inherent structural and anatomical characteristics of each wood species, such as fiber

length, cell wall thickness, and the overall density of the wood. For example, *T. grandis* is known for its dense, interlocked grain structure, which likely contributes to its superior bending resistance and overall mechanical strength. In contrast, *F. chinensis*, which has a lower density and more uniform cellular structure, exhibited comparatively lower bending strength.

These findings align with previous studies that highlighted the role of wood density and fiber arrangement in determining the mechanical properties of wood. Research has shown that wood species with a higher density generally exhibit better mechanical properties, including bending strength and stiffness. However, it is important to note that while higher density often correlates with better performance, other factors such as fiber orientation and cell wall structure also play crucial roles in determining the bending characteristics of wood.

The chemical, physical, and mechanical properties of wood are intrinsically interconnected. Chemically, lignin degradation reduced inter-fiber rigidity, while increased cellulose crystallinity enhanced microfibril alignment. Physically, species-specific traits, such as *F. chinensis*'s high vessel ratio and low density—facilitated greater deformation under stress. Mechanically, the inverse correlation between density and bending deformation (Table 8) underscores how bulk properties modulate chemical treatment efficacy. These findings collectively highlight the need for a holistic approach when selecting species and treatments for bent wood applications, where chemical modifications must align with inherent anatomical and mechanical characteristics to optimize performance.

Effect of softening treatments on bending performance

The softening treatments applied in this study, including water, ammonia, and composite alkali treatments, had a significant impact on the bending performance of the wood samples. Among the three treatments, composite alkali treatment proved to be the most effective in improving the bending strength of the wood, followed by ammonia treatment. This is consistent with findings from earlier studies that suggested the degradation of lignin and hemicellulose during softening treatments could increase the flexibility of the wood, making it more pliable and easier to bend.

The composite alkali treatment, which involved the use of a hydrothermal method combined with additives such as swelling agents and lubricants, helped to degrade the lignin and hemicellulose in the wood, thereby reducing the rigidity of the wood and enhancing its ability to bend without breaking. This treatment not only improved the bending performance but also contributed to a more uniform bending process across the different wood species.

On the other hand, water treatment and ammonia treatment showed less pronounced effects on the bending strength. While these treatments did soften the wood to some extent, they did not achieve the same degree of improvement in bending strength as the composite alkali treatment. This could be due to the fact that water treatment primarily affects the non-crystalline regions of cellulose, whereas ammonia treatment primarily targets lignin degradation. However, without the additional effects of swelling agents or lubricants, these treatments may not have been as effective in enhancing the bending properties.

Comparison with previous studies

The results of this study are consistent with previous research on wood softening and bending processes. Studies have shown that hydrothermal treatment, including both hot water and steam treatment, is effective in softening wood and facilitating bending. However, as highlighted in earlier work, traditional softening methods such as boiling often suffer from slow processing times and high moisture content in the final product, which can limit their practical applications.

In contrast, the composite alkali treatment explored in this study demonstrated its potential as an effective method for improving wood bending properties, aligning with findings from research on ammonia and alkali treatments. These treatments have been shown to effectively degrade lignin and hemicellulose, resulting in enhanced wood flexibility and better bending performance. The use of additives such as swelling agents and lubricants further improves the uniformity of the treatment and the overall quality of the bent wood.

Practical implications and future research directions

The findings of this study have important practical implications for the wood industry, particularly in the production of curved wooden components for furniture and construction. The use of composite alkali treatment for softening wood could be adopted as a standard method for enhancing the bending performance of various wood species, making it more suitable for applications requiring complex shapes and high strength.

Future research should explore the long-term durability of bent wood treated with composite alkali, particularly in terms of its resistance to environmental factors such as moisture, temperature fluctuations, and mechanical stress. Additionally, further studies could investigate the effects of different treatment parameters (*e.g.*, temperature, time, and concentration of additives) on the bending performance of wood, as well as the potential for scaling up this treatment method for industrial applications.

Moreover, future work could also consider a broader range of wood species and explore the synergistic effects of combining multiple treatment methods, such as microwave treatment or chemical modification, to further enhance wood's bending properties and performance in various applications. Future studies should explore the long-term durability of bent wood treated with composite alkali, particularly in terms of its resistance to environmental factors such as moisture and temperature fluctuations.

CONCLUSIONS

- 1. This study systematically investigated the bending behavior of four wood species (F. chinensis, T. grandis, H. brasiliensis, and P. yunnanensis) under hydrothermal and chemical softening treatments. Species-specific anatomical traits (e.g., vessel ratio, fiber length) predominantly governed bending performance variations. T. grandis exhibited superior bending strength due to its dense interlocked grain, while F. chinensis showed the highest bending deformation ratio (h/r = 0.102), which can be attributed to its lower density, higher vessel ratio, and longer fiber length.
- 2. Composite alkali treatment (40% ammonia + 5% ethylenediamine with surfactants) outperformed traditional hydrothermal and ammonia treatments, achieving an 18 to 32% reduction in inter-fiber friction and selective lignin degradation, as confirmed by XRD and FT-IR analyses. This treatment enhanced cellulose crystallinity by 12 to 18% across

- species, facilitating uniform plasticity and structural integrity during bending. Notably, bending deformation stabilized beyond critical thresholds (40% moisture, 120 °C), with optimal performance observed at 6-h treatment durations.
- 3. These findings underscore the potential of compound lye treatments as a cost-effective method for improving the workability of curved wood components in furniture and construction. Future research should focus on optimizing surfactant ratios, exploring hybrid treatments (*e.g.*, microwave-assisted processes), and evaluating long-term durability under environmental stressors. Additionally, extending this methodology to other high-density hardwoods could broaden its industrial applicability.
- 4. By bridging microstructure analysis with mechanical performance, this study advances the rational selection of wood species and treatment protocols, offering actionable strategies for sustainable wood processing and innovation in structural design.

ACKNOWLEDGMENTS

This study was financially supported by the Fujian Provincial Natural Science Foundation Project, titled "Research on the Evolution of the Contact Surface Behavior of Wooden Beam and Column Mortise-and-Tenon Joints in Historic Buildings," grant No. 2024J01834, and the Major Project of Fujian Provincial Social Science Research Base, titled "Research on the Digital Organization and Living Inheritance of Intangible Cultural Heritage in Fujian Province, Focusing on Traditional Craftsmanship," grant No. FJ2023JDZ056.

Competing Interests

The authors declare no conflict of interest.

Author Contributions

Huajie Shen: conceptualization, data curation, funding acquisition, writing—original draft, and writing—review and editing. Caixia Bai: conceptualization, supervision, resources, formal analysis, and writing—review and editing. Fengwu Zhang: methodology, resources, writing—original draft, and writing—review and editing. Yue Sun: formal analysis and writing—review and editing. Xinzhen Zhuo and Rongfeng Ding: data curation, visualization, and writing—review and editing. Donghai Huang: Resources, supervision, and writing—review and editing. Yushan Yang: Supervision, methodology, and writing-review and editing.

REFERENCES CITED

- Aramburu, A. B., de Peres, M. L., Delucis, R. D., and Gatto, D. A. (2022). "Bending quality of three Brazilian hardwoods modified by different hydrothermal treatments," *Cerne* 28. DOI: 10.1590/01047760202228013114
- Bai, R., Wang, W., Chen, M., and Wu, Y. (2024). "Study of ternary deep eutectic solvents to enhance the bending properties of ash wood," *RSC Advances* 14(12), 8090-8099. DOI: 10.1039/D4RA00357H
- Fajdiga, G., Rajh, D., Nečemer, B., Glodez, S., and Sraml, M. (2019). "Experimental and numerical determination of the mechanical properties of spruce wood," *Forests* 10.

- DOI: 10.3390/f10121140
- Gao, Y., Li, L., and Chen, Y. (2023). "Adding gaseous ammonia with heat treatment to improve the mechanical properties of spruce wood," *Holzforschung* 77(6), 416-425. DOI: 10.1515/hf-2022-0179
- Gašparík, M., and Barcík, Š. (2014). "Effect of plasticizing by microwave heating on bending characteristics of beech wood," *BioResources* 9(3), 4808-4820. DOI: 10.15376/biores.9.3.4808-4820
- GB/T 1932-2009 (2009). "Method for determining drying shrinkage of wood," Standards Press of China, Beijing.
- GB/T 1933-2009 (2009). "Method for determining wood density," Standards Press of China, Beijing.
- GB1934.1-2009 (2009). "Method for determining water absorption of wood," Standards Press of China, Beijing.
- GB1934.2-2009 (2009). "Method for determining wood moisture expansion," Standards Press of China, Beijing.
- GB1936.1-2009 (2009). "Test method for bending strength of wood," Standards Press of China, Beijing.
- GB1936.2-2009. (2009). "Method for determination of modulus of elasticity in bending of wood," Standards Press of China, Beijing.
- Huang, D., Shen, H., Zhang, J., Zhuo, X., and Dong, L. (2024). "Effects of hydrothermal-microwave treatment on bending properties of teak in plantation," *Frontiers in Materials* 11, 1278707. DOI: 10.3389/fmats.2024.1278707
- Hussin, T. A. B. R. (2023). "The flexural strength behaviour of balau and chengal timber species using the analysis of modulus of rupture (MOR) and modulus of elasticity (MOE) parameters," *Journal of Engineering & Technological Advances* 8(2), 40-53.
- International Association of Wood Anatomists (IAWA) (2004). *IAWA List of Microscopic Features for Hardwood Identification*, Leiden, Netherlands.
- Kherais, M., Csébfalvi, A., Len, A., Fülöp, A., and Pál-Schreiner, J. (2024). "The effect of moisture content on the mechanical properties of wood structure," *Pollack Periodica* 19(1), 41-46. DOI: 10.1556/606.2023.00917
- Kubík, P., Šebek, F., Hassan Vand, M., Brabec, M., and Tippner, J. (2024). "Fracture predictions in impact three-point bending test of European beech," *Journal of Wood Science* 70(1), 42. DOI:10.1186/s10086-024-02157-x
- Kurul, F., and As, N. (2024). "Visual and machine strength gradings of Scots and red pine structural timber pieces from Türkiye," *BioResources*, 19(3), 4135-4154. DOI: 10.15376/biores.19.3.4135-4154
- Mai, C., Schmitt, U., and Niemz, P. (2022). "A brief overview on the development of wood research," *Holzforschung* 76, 102-119. DOI: 10.1515/hf-2021-0123
- Perçin, O., Yeşil, H., Uzun, O., and Bülbül, R. (2024). "Physical, mechanical, and thermal properties of heat-treated poplar and beech wood," *BioResources* 19(4), 7339-7353. DOI: 10.15376/biores.19.4.7339-7353
- Pestka, A., Kłosowski, P., Lubowiecka, I., and Krajewski, M. (2019, February). "Influence of wood moisture on strength and elastic modulus for pine and fir wood subjected to 4-point bending tests," in: *IOP Conference Series: Materials Science and Engineering* 471(3), p. 032033, IOP Publishing. DOI: 10.1088/1757-899X/471/3/032033
- Ratnasingam, J., Ab Latib, H., Liat, L. C., and Reza Farrokhpayam, S. (2022). "Comparative steam bending characteristics of some planted forest wood species in

- Malaysia," *BioResources* 17(3), 4937-4951. DOI: 10.15376/biores.17.3.4937-4951 Schweingruber, F. H., and Crivellaro, A. (2016). "Comments on the IAWA Hardwood List now available on the web," *IAWA Journal* 37, 369-371. DOI: 10.1163/22941932-20160140
- Shen, H., Qiu, J., Yang, Y., Wang, X., and Wang, Y., (2020). "Anatomical characteristics and physical and mechanical properties analysis of six types of wood," *Journal of Southwest Forestry University (Natural Science)* 40(02), 149-154.
- Sun, W., and Li, J. (2010). "Analysis and characterization of dimensional stability and crystallinity of larch wood after high-temperature heat treatment," *Forest Science* 46(12), 114-118.
- Tong, D., Zhang, Y., and Song, K. (2013). "Comparative analysis of longitudinal compressive and bending properties of hydrothermal-treated juvenile and mature elm wood," *BioResources* 8(1), 383-394.
- Wang, X., Shen, H., Wang, Y., Yang, Y., and Qiu, J. (2019). "Effect of ammonia and hydrothermal treatment on chemical properties of teak flexure in plantations," *Light Industry Science and Technology* (04), 46-48.
- Weigl, M., Müller, U., Wimmer, R., and Hansmann, C. (2012). "Ammonia vs. thermally modified timber—Comparison of physical and mechanical properties," *European Journal of Wood and Wood Products* 70(1), 233-239. DOI: 10.1007/s00107-011-0537-z
- Wu, Y., Zhu, J. G., Qi, Q., and Cui, L. N. (2022). "Research progress of solid wood bending softening technology," *Wood Research* 67, 1056-1073. DOI: 10.37763/wr.1336-4561/67.6.10561073
- Xia, Q., Liu, Y., Meng, J., Cheng, W., Chen, W., Liu, S., Liu, Y., Li, J., and Yu, H. (2018). "Multiple hydrogen bond coordination in three-constituent deep eutectic solvents enhances lignin fractionation from biomass," *Green Chemistry* 20(12), 2711-2721. DOI: 10.1039/C8GC00900G
- Yang, Y., Shen, H., Wang, X., Wang, Y., and Qiu, J. (2019). "Study on the microstructure damage mechanism of steam molded bent poplar wood," *Shandong Forestry Science and Technology* (05), 1-5.
- Zhang, W., Bao, M., Sun, W., Huang, L., and Cheng, L. (2021). "Effect of ammonia fumigation treatment on wood color and chemical composition," *International Journal of Polymer Science* 2021(1), article 5550800. DOI: 10.1155/2021/5550800

Article submitted: February 16, 2025; Peer review completed: March 16, 2025; Revised version received: March 19, 2025; Accepted: April 17, 2025; Published: April 30, 2025. DOI: 10.15376/biores.20.2.4635-4661